

# Pointing Algorithm for Reentry Orbit Injection with Uncontrolled Last Stage

Flávio Eler de Melo<sup>1,\*</sup>, Waldemar de Castro Leite Filho<sup>2</sup>, Hilton Cleber Pietroboim<sup>2</sup>

<sup>1</sup>Embraer S.A.- São José dos Campos/SP – Brazil

<sup>2</sup>Instituto de Aeronáutica e Espaço – São José dos Campos/SP – Brazil

**Abstract:** *An essential requirement for a launcher with uncontrolled last stage is to compute the ignition time of that stage and its attitude, in order to obtain a proper orbit transfer from a nonpropelled trajectory to a desired orbit, since such stage it cannot change its velocity profile and its direction. This article presents an algorithm that allows achieving the proper conditions to inject a vehicle with uncontrolled last stage into a descent Keplerian trajectory, in order to permit its reentry through the Earth's atmosphere with strictly defined conditions of radius, velocity, and flight path angle at the entry interface. These specific conditions impose requirements to the configuration, performance, and trajectory of the launcher. This strategy considers that the total energy is applied instantly for the reentry orbit injection. Impulsive ignition time and necessary attitude for the last stage are obtained based on orbital parameters, having a match between the nonpropelled and reentry orbits, and boundary conditions at the initial state and at the entry interface. Impulsive ignition time was corrected for compensating the impulsive assumption and the calculated attitude related to an inertial frame. The obtained results show the efficiency of the algorithm involving reentry missions with uncontrolled last stage, as the Sharp Edge Flight Experiment (SHEFEX) program.*

**Keywords:** *Algorithms, Orbit transfer vehicles, Pointing control systems, Reentry guidance, Reentry vehicle, Trajectory analysis.*

## INTRODUCTION

Some reentry experiments for investigating aerothermodynamics performance and control during hypersonic flight have been conducted to provide design guidelines for future reusable space transportation systems or hypersonic vehicles. Such studies evaluated the design aspects of aerothermodynamics profile, materials, structure, and hypersonic flight control. The Sharp Edge Flight Experiment (SHEFEX) program is the main instance of such reentry missions. A launch vehicle for a reentry object is typically composed of two or more stages. Both the SHEFEX 1 and 2 are propelled by a final second stage configuration, based on the two-stage Brazilian solid propellant rocket VS-40 (Theil *et al.*, 2008).

Missions are programmed with sequenced events and they are guided based on nominal trajectories. In an uncontrolled last stage configuration, the last stage does not control either

velocity or attitude, being only the vehicle spin responsible for stabilizing. Given the dispersions and disturbances on the flight, the nominal pre-programmed attitude reference and ignition time for the last stage could not fulfill the conditions for a sufficiently accurate orbit transfer.

Only between the penultimate stage burnout and the last stage ignition, the launch vehicle is practically subject only to the gravitational force, fact that describes a Keplerian orbit. This is a coast phase, where the pitch-over (directional maneuver) and spin-up maneuvers shall happen. The ignition of the last stage changes the Keplerian trajectory to inject the vehicle into a descent one for the reentry.

The pointing algorithm described here is based on the algorithms provided by Leite Filho (1994), Nepomuceno and Leite Filho (2011), and Pietroboim and Leite Filho (2011). Leite Filho (1994) and Nepomuceno and Leite Filho (2011) developed an algorithm to obtain a proper transfer from a Keplerian orbit to a circular one, with both defined radius and inclination, while Pietroboim and Leite Filho (2011) did not worry about the eccentricity of the orbit, but to ensure that the

Received: 23/02/12

Accepted: 13/05/12

\*author for correspondence: flavio.melo@embraer.com.br

Av. Brig. Faria Lima, 2170, Putim – CEP:12227-901 - São José dos Campos – SP/Brazil

injection altitude of the satellite corresponded to the perigee of the final orbit. On the other hand, differently from the two algorithms mentioned previously, this algorithm presents a pointing strategy to permit the reentry of the satellite through the Earth's atmosphere with strictly defined conditions of radius, velocity, and flight path angle at the entry interface.

A pointing algorithm can be run in the beginning of the coast phase to obtain a proper transfer from the actual orbit to the desired one. The orbit transfer is assumed as an impulsive transfer, which means the total energy of the last stage is applied as an impulse. Based on actual navigation data (time, position, and velocity), characteristics of the last stage (burning time, increment of position and velocity due to its burning) and reentry conditions, the impulsive ignition time and the necessary attitude that the last stage must be pinpointed in this time are calculated. Impulsive ignition time is then corrected for compensating the impulsive assumption, by means of an energetic balance (Robbins, 1966, Leite Filho, 1994), and the calculated attitude is related to an inertial frame (Leite Filho, 1994).

The pointing algorithm presented here was performed once, assuming that no disturbance changed the initial Keplerian orbit. Also, the algorithm was performed just after the penultimate stage separation to avoid that the increasing inertial sensor errors could affect significantly the calculations accuracy.

Some tradeoffs must be taken into consideration when selecting one of the possible orbit transfers. The impulsive orbit transfer may occur in the ascent section of the coast phase trajectory or in the descent one, as can be seen in Fig. 1. For preventing disturbances that may degrade the accuracy of the injection into the reentry trajectory, it is better that the injection occurs in the ascent section of the coast phase orbit. On the other hand, in case the orbit transfer occurs in the

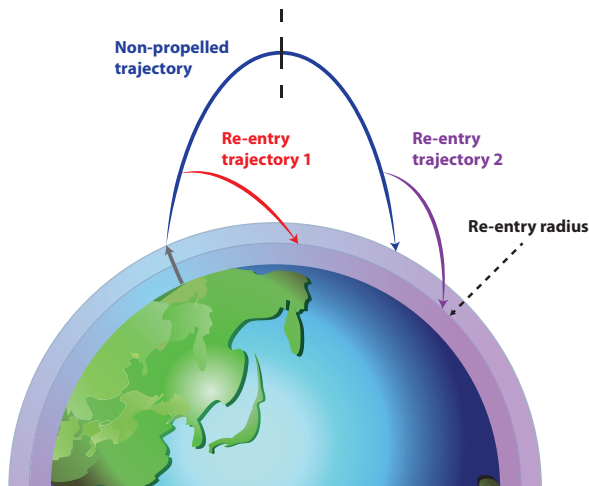


Figure 1. Impulsive orbit transfer for a reentry mission.

descent section, the amount of minimum energy necessary for the transfer into the reentry trajectory will be slightly smaller, which means that less propellant would be necessary for an injection from the descent section.

## GENERAL FORMULATION

The general problem formulation to establish the necessary conditions for an orbit transfer at  $t=t_i$  will be recalled from Leite Filho (1994). The instant  $t_i$  is the ignition time of the last stage for an hypothetical impulsive orbit transfer.

The motion of the vehicle's center of gravity during the coast phase and burning of the last stage, follow the dynamics as in Eq. 1:

$$\ddot{\vec{R}} = \vec{g}(R) + \Gamma(t) \cdot \vec{\Delta}, \quad (1)$$

where  $\vec{g}$  is the gravitational acceleration and  $\vec{\Delta}$  is the unit vector in the thrust direction.  $\Gamma$  is the propulsive acceleration given by Eq. 2:

$$\Gamma(t) = \frac{T(t-t_{ig})}{m_s + m_p(t-t_{ig})}, \quad (2)$$

where  $T(t-t_{ig})$  is the thrust,  $m_s$  is the structural mass and  $m_p(t-t_{ig})$  is the propellant mass of the last stage with ignition time  $t_{ig}$ .  $T(\cdot)$  and  $m_p(\cdot)$  are known functions. The solution to Eq. 1 can be formulated by Eqs. 3 and 4:

$$\vec{v} = \vec{V}_{ig} + \Delta V \cdot \vec{\Delta} + \Delta \vec{V}_g; \quad (3)$$

$$\vec{R} = \vec{R}_{ig} + (t-t_{ig}) \cdot \vec{V}_{ig} + \Delta R \cdot \vec{\Delta} + \Delta \vec{R}_g; \quad (4)$$

where,

$$\Delta V = \int_{t_{ig}}^t \Gamma(\lambda) d\lambda, \quad (5)$$

$$\Delta R = \int_{t_{ig}}^t \Delta V(\lambda) d\lambda, \quad (6)$$

$$\Delta \vec{V}_g = \int_{t_{ig}}^t \frac{\mu \vec{R}(\lambda)}{R(\lambda)^3} d\lambda, \quad (7)$$

$$\Delta \vec{R}_g = \int_{t_{ig}}^t \Delta \vec{V}_g(\lambda) d\lambda, \quad (8)$$

so that  $\Delta V$  and  $\Delta R$  are increments of velocity and position due to propulsive acceleration, and  $\Delta \vec{V}_g$  and  $\Delta \vec{R}_g$  are increments of velocity and position due to gravitational acceleration, respectively (Eqs. 5 to 8).

The increment of angular momentum due to the last stage burning is provided by Eq. 9:

$$\Delta \vec{H} = \vec{R} \times m \vec{V} - \vec{R}_{ig} \times m_{ig} \vec{V}_{ig} \tag{9}$$

Following Leite Filho (1994), by substituting Eqs. 3 and 4 into Eq. 9, and considering that the gravity loss has nearly the same direction as  $R_{ig}$  and the distance travelled during the thrust is negligible in comparison to the radius vector, i.e.,  $\Delta \vec{R}g \approx (t_f - t_{ig}) \Delta \vec{V}_g$ , the final equation is as Eq. 10:

$$\Delta \vec{H} = m \left\{ \vec{R}_{ig} + \left[ (t_f - t_{ig}) - \frac{\Delta R}{\Delta V} \right] \cdot (\vec{V}_{ig} + \Delta \vec{V}_g) \right\} \times \Delta V \cdot \vec{\Delta} + m \vec{R}_{ig} \times \vec{V}_{ig} - m_{ig} \vec{R}_{ig} \times \vec{V}_{ig}, \tag{10}$$

where,  $t_f$  is the burnout time of the last stage. Equation 10 can be rearranged as Eq. 11:

$$\Delta \vec{H} = m \vec{R}_I \times \Delta V \cdot \vec{\Delta} + (m - m_{ig}) \vec{R}_{ig} \times \vec{V}_{ig} \tag{11}$$

where,

$$\vec{R}_I = \vec{R}_{ig} + \left[ (t_f - t_{ig}) - \frac{\Delta R}{\Delta V} \right] \cdot (\vec{V}_{ig} + \Delta \vec{V}_g) \tag{12}$$

Equation 11 is interpreted as an orbital change due to an impulsive thrust applied at  $R_I$ . By the principle of conservation of angular moment (Eq. 13):

$$\Delta \vec{H} = m \vec{R}_I \times (\vec{V}_I + \Delta V \cdot \vec{\Delta}) - m_{ig} \vec{R}_{ig} \times \vec{V}_{ig} \tag{13}$$

Equation 12 shows that  $R_I$  will occur  $\eta$  seconds after  $t_{ig}$ , where

$$\eta = (t_f - t_{ig}) - \frac{\Delta R}{\Delta V}, \tag{14}$$

and it shows that the impulsional shot in  $R_I$ , with direction  $\vec{\Delta}$ , is equivalent to the actual thrust started in  $t_{ig}$  with the same direction. This equivalence is corrected by the factor  $\eta$ , which compensates the impulsional assumption for the ignition time  $t_f$ . Therefore, the actual thrust is applied at the following time (Eqs. 14 and 15):

$$t_{ig} = t_I - \eta. \tag{15}$$

**CONDITIONS FOR IMPULSIVE ORBIT TRANSFER**

As illustrated by Fig. 2, the orbit transfer of a launch vehicle last stage from the coast phase to the reentry orbit might be obtained by applying an increment of velocity  $\Delta V$  in a direction described by  $\alpha$ , and by constraining the solution to the initial condition of radius ( $R_0$ ), velocity ( $V_0$ ) and flight path angle ( $\gamma_0$ ) at the beginning of the coast phase and to the reentry conditions

of radius ( $R_R$ ), velocity ( $V_R$ ), and flight path angle ( $\gamma_R$ ).

When applying the increment of velocity in the direction described by  $\alpha$ , the coast phase and the reentry trajectories are related by Eqs. 16 and 17:

$$v_1 \sin \gamma_1 + \Delta V \sin \alpha = V_2 \sin \gamma_2; \tag{16}$$

$$V_1 \cos \gamma_1 + \Delta V \cos \alpha = V_2 \cos \gamma_2. \tag{17}$$

Since the last stage's coast phase orbit is Keplerian (Chobotov, 2002, Bate *et al.*, 1971), the *vis viva* equation and the angular momentum conservation principle produces Eqs. 18 and 19:

$$RV_1 \cos \gamma_1 = R_0 V_0 \cos \gamma_0 \tag{18}$$

and

$$V_1^2 = \frac{2\mu}{R} - \frac{\mu}{a_1}, \tag{19}$$

where,

$$\gamma_0 = \arcsin \left( \frac{\vec{R}_0 \cdot \vec{V}_0}{|\vec{R}_0| \cdot |\vec{V}_0|} \right). \tag{20}$$

The parameter  $\mu$  is the product of the Earth's mass with the gravitational constant. The resulting reentry orbit is also Keplerian, creating Eqs. 21 and 22:

$$RV_2 \cos \gamma_2 = R_R V_R \cos \gamma_R \tag{21}$$

$$V_2^2 = \frac{2\mu}{R} - \frac{\mu}{a_2}. \tag{22}$$

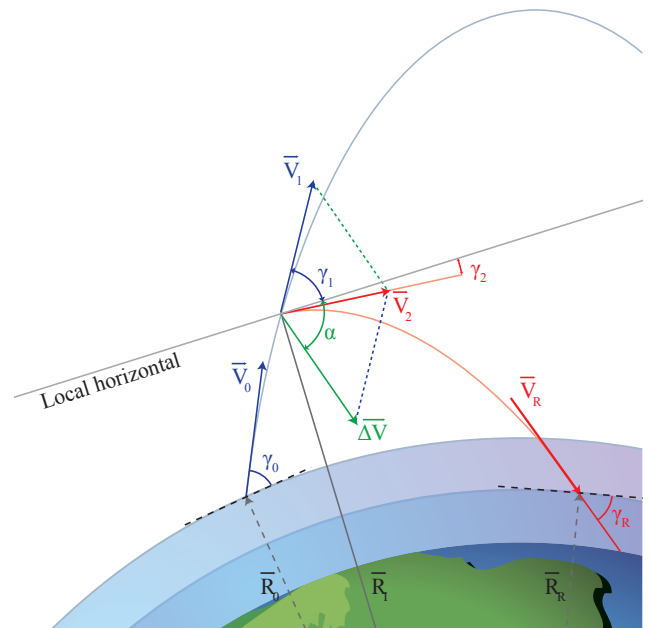


Figure 2. Vector diagram of the orbit transfer.

By defining a specific angular momentum  $h_i = |\vec{H}_i|/m_i$ , Eqs. 18 and 21 can be rewritten as Eqs. 23 and 24:

$$h_1 = RV_1 \cos \gamma_1 = R_0 V_0 \cos \gamma_0; \tag{23}$$

$$h_2 = RV_2 \cos \gamma_2 = R_R V_R \cos \gamma_R \tag{24}$$

Rearranging Eqs. 16 and 17 to isolate  $\Delta V$ , then squaring and adding one to another, yields Eq. 25:

$$\Delta V^2 = V_1^2 + V_2^2 - 2V_1V_2(\cos \gamma_1 \cos \gamma_2 + \sin \gamma_1 \sin \gamma_2). \tag{25}$$

Based on Eqs. 23 and 24, Eq. 25 can be rearranged and manipulated by proceeding the substitutions  $V_1 \cos \gamma_1 = h_1/R$ ,  $V_2 \cos \gamma_2 = h_2/R$ ,  $V_1 \sin \gamma_1 = \sqrt{V_1^2 - (h_1/R)^2}$ , and  $V_2 \sin \gamma_2 = \sqrt{V_2^2 - (h_2/R)^2}$  in order to achieve Eq. 26:

$$V_1^2 + V_2^2 - 2 \frac{h_1 h_2}{R^2} - \Delta V^2 = 2 \sqrt{V_1^2 - \left(\frac{h_1}{R}\right)^2} \sqrt{V_2^2 - \left(\frac{h_2}{R}\right)^2}. \tag{26}$$

Substituting Eqs. 19 and 22 into Eq. 26, then squaring and rearranging it, a cubic equation in  $R$  is obtained as showed by Eq. 27:

$$A_\gamma \cdot R^3 + B_\gamma \cdot R^2 + C_\gamma \cdot R + D_\gamma = 0 \tag{27}$$

where,

$$\begin{aligned} A_\gamma &= \frac{\mu^2 a_1^2 - 2\mu^2 a_1 a_2 + 2\Delta V^2 \mu a_1^2 a_2 + \mu^2 a_2^2}{a_1^2 a_2^2} \\ &\quad + \frac{2\Delta V^2 \mu a_1 a_2^2 + \Delta V^4 a_1^2 a_2^2}{a_1^2 a_2^2}, \\ B_\gamma &= -8\Delta V^2 \mu; \\ C_\gamma &= \frac{-4\mu a_1^2 a_2 h_1^2 + 4\mu a_1^2 a_2 h_1 h_2 + 4\mu a_1 a_2^2 h_1 h_2}{a_1^2 a_2^2} \\ &\quad + \frac{4\Delta V^2 a_1^2 a_2^2 h_1 h_2 - 4\mu a_1 a_2^2 h_2^2}{a_1^2 a_2^2}, \\ D_\gamma &= \frac{8\mu a_1^2 a_2^2 h_1^2 - 16\mu a_1^2 a_2^2 h_1 h_2 + 8\mu a_1^2 a_2^2 h_2^2}{a_1^2 a_2^2}. \end{aligned} \tag{28}$$

From the three roots of Eq. 27, only one real root is appropriate for the problem solution. The chosen method for finding the appropriate real root is a generalized method (Birkhoff and Mac-Lane, 1998, Weisstein, 2011) based on the Viète trigonometric solution (Eq. 29):

$$R_l = -\frac{1}{3} \cdot \frac{B_\gamma}{A_\gamma} + 2 \cdot \sqrt{\frac{|p|}{3}} \cdot \cos\left(\frac{1}{3} \arccos(C)\right) \tag{29}$$

where,

$$\begin{aligned} p &= \frac{1}{3} \left( 3 \frac{C_\gamma}{A_\gamma} - 2 \frac{B_\gamma^2}{A_\gamma^2} \right); \\ q &= \frac{1}{27} \left( 9 \frac{B_\gamma C_\gamma}{A_\gamma^2} - 27 \frac{D_\gamma}{A_\gamma} - 2 \frac{B_\gamma^3}{A_\gamma^3} \right); \\ C &= \frac{1}{2} q \cdot \sqrt{\left(\frac{3}{|p|}\right)^3}. \end{aligned} \tag{30}$$

In the generalized method presented by Birkhoff and Mac-Lane (1998), if  $p > 0$ , the real roots are found from the hyperbolic-sine triple-angle identity. If  $p < 0$  and  $|C| \geq 1$ , the real roots are calculated based on the hyperbolic-cosine triple-angle identity. If  $p < 0$  and  $|C| < 1$ , the real roots are calculated based on the cosine triple-angle identity (Viète solution). For the trajectory characteristics considered by this paper, the physically possible solutions are defined for  $p < 0$  and  $|C| < 1$ , leading to the solution described by Eq. 29.

As a verification method, it is worth noting that the solution is only practical for a specific range of  $R_\gamma$ . This range is obtained based on the fact that  $R_\gamma$  cannot be smaller than the radius of the coast phase beginning. Additionally, it cannot be greater than the solution where the reentry orbit locus has only one coincident point with the coast phase orbit locus. The practical range for the  $R_\gamma$  solutions can be established by Eq. 31:

$$R_{min} = R_0 < R < R_{max} = a_1(1 + e_1) \tag{31}$$

Also, minimum and maximum possible reentry angles depend on  $h_2$  at the limit radius for a successful orbit transfer. By rearranging Eq. 27 for isolating powers of  $h_2$ , minimum and maximum  $h_2$  at the limit radius can be calculated by a quadratic equation of the form given by Eq. 32:

$$A_h \cdot h_2^2 + B_h \cdot h_2 + C_h = 0 \tag{32}$$

where,

$$\begin{aligned} A_h &= 4\mu \left( 2 - \frac{R}{a_1} \right) \frac{1}{R^3} \Big|_{R=R_{min}, R_{max}}; \\ B_h &= \frac{4\{R\mu a_2 + a_1[R\mu + (R\Delta V^2 - 4\mu)a_2]\}h_1}{R^3 a_1 a_2} \Big|_{R=R_{min}, R_{max}}; \\ C_h &= \Delta V^4 - \frac{8\Delta V^2 \mu}{R} + \frac{\mu^2}{a_1^2} + \frac{2\mu}{a_1} \left( \Delta V^2 - \frac{\mu}{a_2} \right) \\ &\quad + \frac{\mu}{a_2^2} \left\{ \mu + 2a_2 \left[ \Delta V^2 - \frac{2(R - 2a_2)h_1^2}{R^3} \right] \right\} \Big|_{R=R_{min}, R_{max}} \end{aligned} \tag{33}$$

Based on Eq. 24, maximum and minimum reentry angles are calculated by Eq. 34:

$$\gamma_R \Big|_{min, max} = \arccos\left(\frac{h_2 \Big|_{max, min}}{R_R V_R}\right). \tag{34}$$

The flight path angle at the entry interface has the same absolute value as the reentry angle calculated by Eq. 34.

Given the value of the radius  $R_p$ , an impulsive shot must be carried out at it to inject the last stage into the reentry orbit with flight path  $\gamma_2$ . The direction of the impulsive shot is defined by the angle as in Eq. 35:

$$\alpha = \pm \frac{1}{R_i} \arccos\left(\frac{h_2 - h_1}{\Delta V}\right). \quad (35)$$

Two angles, one positive and another negative, can be achieved from Eq. 35, providing two solutions of reentry trajectories that satisfy the same conditions. One solution is for the orbit transfer from the ascent section of the coast phase, and the other one is for the transfer from the descent section. It is worth to note that this study can support analyses for selecting an appropriate launch vehicle for the reentry mission, as the minimum required  $\Delta V$  that satisfies the required conditions at the entry interface depends on the energy of the launch vehicle at the coast phase trajectory. Manipulating Eq. 27 for isolating powers of  $\Delta V$ , the smallest  $\Delta V$  at the minimum, and maximum possible radius for the orbit transfer can be obtained by using the resulting quadratic Eq. 36:

$$A_v \cdot \Delta V^4 + B_v \cdot \Delta V^2 + C_v = 0 \quad (36)$$

where,

$$A_v = 1;$$

$$B_v = \frac{2R^3\mu a_1^2 a_2 + 2R^3\mu a_1 a_2^2 - 8R^2\mu a_1^2 + 4Ra_1^2 a_2^2 h_1 h_2}{R^3 a_1^2 a_2^2} \Big|_{R=R_{min}, R_{max}};$$

$$C_v = \frac{1}{R^3 a_1^2 a_2^2} [R^3 \mu^2 a_1^2 - 2R^3 \mu^2 a_1 a_2 + R^3 \mu^2 a_2^2 + 8\mu a_1^2 a_2^2 h_1^2 - 16\mu a_1^2 a_2^2 h_1 h_2 + 4R\mu a_1 a_2^2 (h_1 - h_2) h_2 + 8\mu a_1^2 a_2^2 h_2^2 + 4R\mu a_1^2 a_2 h_1 (h_2 - h_1)] \Big|_{R=R_{min}, R_{max}}. \quad (37)$$

As mentioned, the orbit transfer maneuver can be proceeded in the ascent section of the coast phase trajectory or in the descent one, but considering the accuracy degradation in guidance due to disturbances and excessive downrange, it is suggested that an impulsive shot in the ascent section would be the best option.

## IGNITION TIME

Taking into consideration Leite Filho (1994), the instant when the impulsive shot is carried out is related to the time interval that the vehicle last stage takes from  $R_0$  to  $R_f$ . Expressing the ignition time in terms of the eccentric anomaly  $E$

(Cornelisse *et al.*, 1979, Leite Filho, 1994) and correcting the impulsive shot ignition time according to Eq. 15, the actual ignition time is (Eq. 38):

$$t_{ig} = \sqrt{\frac{a_1^3}{\mu} [(E_f - E_0) - e_1 (\sin E_f - \sin E_0)]} + \frac{\Delta R}{\Delta V} - \tau + t_0, \quad (38)$$

where,  $\tau = t_f - t_{ig}$  is the burning time of the last stage. The eccentric anomaly is given by Eq 39:

$$E_j = \arccos\left(\frac{a_1 - R_j}{a_1 e_1}\right)_{j=0,f}, \quad (39)$$

the eccentricity of the coast phase ascent trajectory is showed by Eq. 40:

$$e_1 = e_0 = \sqrt{\left(\frac{R_0 \cdot V_0^2}{\mu} - 1\right)^2 \cdot \cos^2 \gamma_0 + \sin^2 \gamma_0}, \quad (40)$$

and its semi-major axis is described by Eq. 41:

$$a_1 = a_0 = \frac{\mu}{\frac{2\mu}{R_0} - V_0^2}. \quad (41)$$

## RELATION TO THE INERTIAL FRAME

The formulation presented so far is related to the flight plane. The vehicle pitch angle  $\Phi$  related to the flight plane is presented herein as given by Leite Filho (1994), using Fig. 3 as reference.

The pitch angle reported to the flight plane can be expressed as Eq. 42:

$$\Phi = -\frac{\pi}{2} + \sigma - \Delta\Theta - \alpha. \quad (42)$$

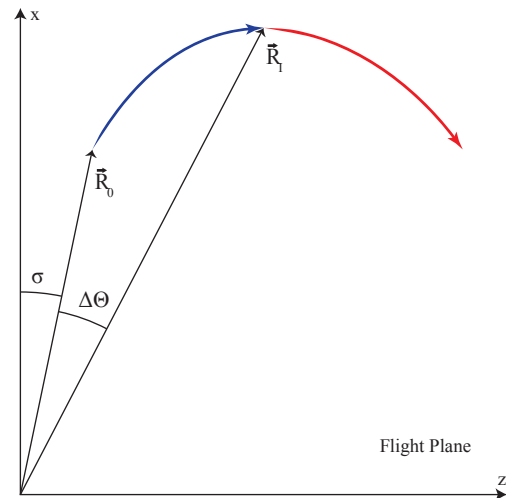


Figure 3. Trajectory related to the flight plane.

The angle between the local vertical direction at the launch site and the one at the coast phase beginning can be calculated by Eq. 43:

$$\sigma = \arccos\left(\frac{\vec{R}_{launch} \cdot \vec{R}_0}{|\vec{R}_{launch}| \cdot |\vec{R}_0|}\right), \quad (43)$$

where,  $\vec{R}_{launch} = (R_e + h_{launch})\hat{i}_x$  is the radius (position) at the launch site considering the mean Earth's radius  $R_e$ , height at the launch site  $h_{launch}$ , and the local vertical direction  $x$  at the launch site is defined by an unit vector  $\hat{i}_x$ .

By calculating the angular argument variation of the coast phase trajectory related to the perigee, based on the ellipsis equation in polar coordinates, the angle  $\Delta\theta$  can be obtained by Eq. 44:

$$\Delta\theta = \arccos\left\{\frac{1}{e_1}\left[\frac{a_1}{R_l}(1 - e_1^2) - 1\right]\right\} - \arccos\left\{\frac{1}{e_1}\left[\frac{a_1}{R_0}(1 - e_1^2) - 1\right]\right\}. \quad (44)$$

In order to refer the pitch angle to the navigation frame, the relation between both frames must be considered as follows. The Euler angles that define the direction of  $\vec{\Delta}$ , to which the last stage must be shot, are expressed by Eqs. 45 and 46:

$$\theta = \arctan(-T_z/T_x) - \pi; \quad (45)$$

$$\psi = \arcsin(T_y); \quad (46)$$

where,

$$\begin{aligned} T_x &= \cos i \cdot \cos \Omega \cdot \cos \Phi - \sin \Omega \cdot \sin \Phi, \\ T_y &= \sin i \cdot \cos \Phi, \\ T_z &= -\cos i \cdot \sin \Omega \cdot \cos \Phi - \cos \Omega \cdot \sin \Phi, \end{aligned} \quad (47)$$

for the right ascension of the ascending node  $\Omega$  and the inclination  $i$  (Cornelisse *et al.*, 1979) given by Eq. 48:

$$\cos i = \frac{\vec{u}_y \cdot \vec{D}}{|\vec{D}|} = \frac{D_y}{|\vec{D}|}, \quad (48)$$

$$\tan \Omega = \frac{D_y}{D_x}; \quad (49)$$

where,  $\vec{D} = \vec{V} \times \vec{R}$ .

## POINTING ALGORITHM

The pointing algorithm, to define the ignition time  $t_{ig}$  and the direction ( $\theta$  and  $\psi$ ) of the shot for injecting the vehicle

last stage into the required reentry trajectory, follows the steps listed as following:

- acquisition of initial conditions  $t_0$ ,  $R_0$ ,  $V_0$  in navigation frame and assignment of reentry conditions  $R_R$ ,  $V_R$  and  $\gamma_R$ ;
- calculation of orbit parameters  $\gamma_0$  (Eq. 20),  $a_1$  (Eq. 41),  $e_1$  (Eq. 40),  $E_l$  (Eq. 39), and  $a_2$  (Eq. 41 for  $R_R$ ,  $V_R$ );
- calculation of orbit transfer radius  $R_l$  (Eq. 23, 24, 28, 29, 30) and validation of calculations using Eq. 31 to 34;
- calculation of ignition time  $t_{ig}$  (Eq. 38);
- calculation of pitch angle in the flight plane  $\Phi$  (Eqs. 35, 42, 43, 44);
- calculation of Euler angles expressed into the navigation frame  $\theta$  and  $\psi$  (Eq. 45 to 49).

This algorithm shall transfer the vehicle to the required reentry orbit meeting conditions  $R_R$ ,  $V_R$  and  $\gamma_R$  at the entry interface.

## SIMULATION RESULTS

Simulations to verify the compliance of orbit injection to the required reentry conditions based on initial data, were performed for three different sets of established reentry conditions, as shown in Table 1.

The initial radius  $R_0$ , as shown in Table 1, was set to the nominal apogee height for the reentry trajectory of SHEFEX-2, according to its mission profile presented in Table 2 (Theil *et al.*, 2008). The initial velocity  $V_0$  and flight path  $\gamma_0$  were determined by recalling three simulation cases executed by Leite Filho (1994) for the Brazilian Satellite Launcher Vehicle, which is based on the rocket engines S-40TM and S-44, similar to the ones used for the SHEFEX-2 launch vehicle.

In general, the reentry mission objectives and the design characteristics of the reentering object determine the velocity  $V_R$  and the reentry angle  $\gamma_R$  at the entry interface. The reentry

Table 1. Flight data.

	Flight A	Flight B	Flight C
Initial conditions			
$R_0$ (km)		6578.000	
$V_0$ (m/s)	5385.719	5580.349	5352.683
$\gamma_0$ (°)	31.21	33.01	30.13
Reentry conditions			
$R_R$ (km)		6500.000	
$V_R$ (m/s)	3400.000	3740.000	4080.000
$\gamma_R$ (°)	25.00	45.00	70.00

Table 2. Specifications of SHEFEX-2 launcher configurations.

Payload	350 kg
Apogee	200 km
Downrange	1150 km
Maximum speed	Mach 10 – 12
Stages	2
Reentry angle	25°

radius  $R_R$  is determined by using NASA's mission control, which adopts 400,000 feet (122 km) as the reentry altitude (Jones and Crawford, 1974, Thompson, 2009). As presented in Table 1, three reentry velocities were chosen to cover the maximum speed range of the SHEFEX-2 mission: Mach ( $M_R$ ) of 10, 11 and 12, respectively, in accordance with Table 2. The reentry angles were set to cover a wide range of feasible solutions, and they were consistent with the SHEFEX-2 specifications in order to test the effectivity of the algorithm:  $\gamma_R$  of 25°, 45°, and 70°.

$\Delta V$  was estimated from temporal mass and thrust curves for the Brazilian Satellite Launcher Vehicle's S-44 engine, which is similar to the second stage of the SHEFEX-2 experiment.

The results of the algorithm application for calculating the radius to the orbit transfer  $R_p$ , the direction of shot in the flight plane  $\alpha$ , and the impulsive ignition time  $t_p$ , are presented in Table 3.

Table 3 presents the simulation results for injections into reentry trajectories by the application of the algorithm

Table 3. Simulation results.

	Flight A	Flight B	Flight C
	Results		
$R_I$ (km)	6628.3040	6935.539	7223.7562
$t_I _{\text{ascent phase}}$ (s)	18.39	134.69	455.80
$t_I _{\text{descent phase}}$ (s)	1013.47	1032.40	534.85
$\alpha$ (°)	±117.99	±126.42	±153.69
$V_1$ (m/s)	5299.642	4989.252	4219.802
$\gamma_1$ (°)	±30.39	±27.18	±2.78
$V_2$ (m/s)	3030.831	2507.118	2087.66
$\gamma_2$ (°)	±4.42	±8.66	±53.03
	Limits		
$R_{\min}$ (km)		6578.000	
$R_{\max}$ (km)	7279.660	7438.025	7227.790
$\gamma_{R,\min}$ (°)	19.16	16.70	16.67
$\gamma_{R,\max}$ (°)	78.93	79.89	68.87
$\Delta V_{\min} _{R_{\min}}$ (m/s)	2974.870	3192.1237	2293.384
$\Delta V_{\min} _{R_{\max}}$ (m/s)	3301.326	3301.326	3301.326

proposed herein, for the three flights specified in Table 1. The results clearly show that the pointing algorithm produces feasible solutions for orbit transfers to reentry trajectories, ensuring that the required conditions are met at the entry interface. The results are suitable for orbit transfers, both from ascent or descent sections of the coast phase trajectory.

The calculated limits for  $R_p$ ,  $\gamma_R$  and  $\Delta V$  provide means to validate the pointing algorithm solutions, in order to avoid unfeasible orbit transfers. Also, the limits allow an evaluation during the preliminary mission design and programming to aid the selection and configuration of the launch vehicle.

Figure 4 shows the simulation results for injections into reentry trajectories, by applying the pointing algorithm for conditions established in Table 1. Figure 5 shows the orbit transfer for  $M_R = 11$  and  $\gamma_R = 45^\circ$ , presenting in details the intersection of the coast phase orbit with the possible reentry trajectories, which met the specified conditions at the entry interface.

As it can be seen by Figs. 4 and 5, the proposed algorithm ensures that the required reentry conditions are met, given the established initial conditions at the beginning of the coast phase.

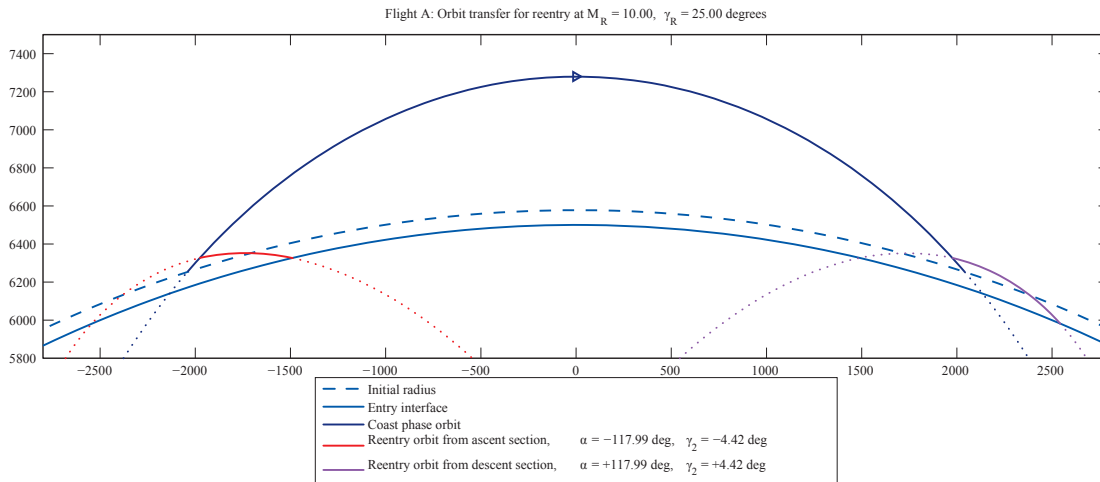
## CONCLUSIONS

Differently of the pointing algorithms described in Leite Filho (1994), Pietrobon and Leite Filho (2011), this paper presented an algorithm that permits the reentry of a vehicle with uncontrolled last stage through the Earth's atmosphere, with strictly defined conditions of radius, velocity and flight path angle at the entry interface.

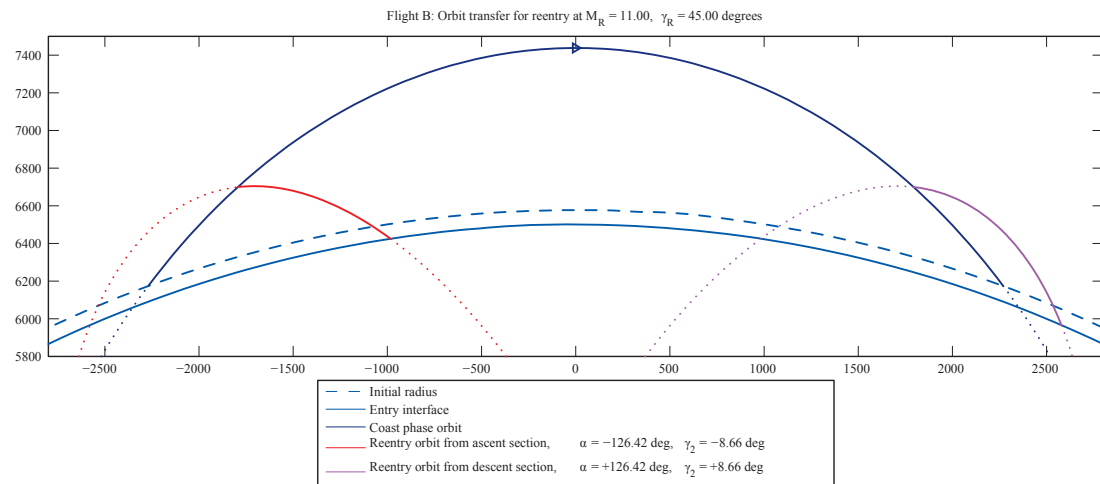
Simulations showed that the pointing algorithm provides an efficient approach to guarantee that the orbit transfer into a required reentry orbit will meet the specified conditions at the entry interface. The obtained results show the efficiency of the algorithm by providing important engineering results related to reentry missions with uncontrolled last stage, as the SHEFEX research program.

Other important results are the condition analyses and limits for the orbit transfer. These analyses allowed a preliminary evaluation during the mission design and provided a guideline for the selection and configuration of an appropriate launch vehicle.

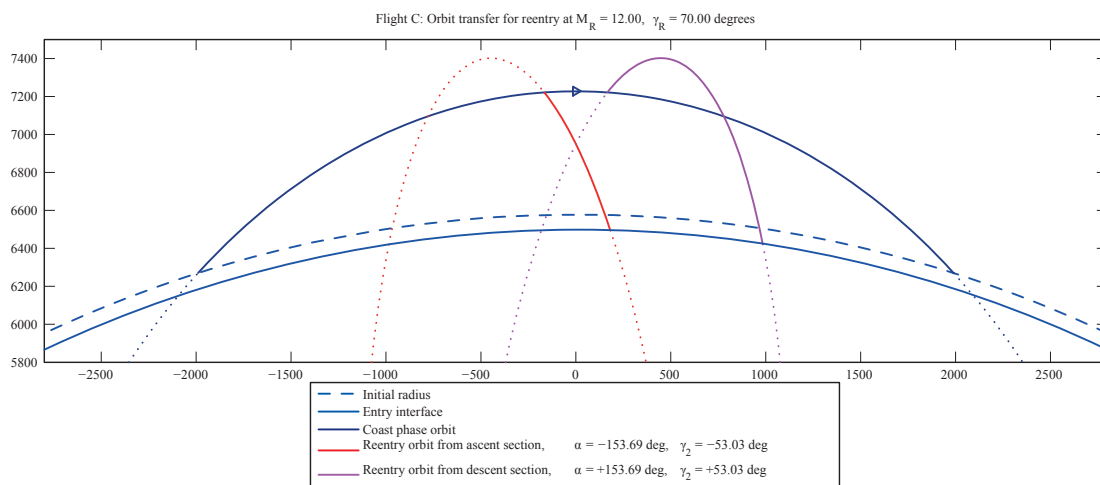
Moreover, the algorithm presented here is just simple to permit its real time implementation into the onboard computer and to provide a successful mission.



(a) Flight A



(b) Flight B



(c) Flight C

Figure 4. Simulated orbit transfers.

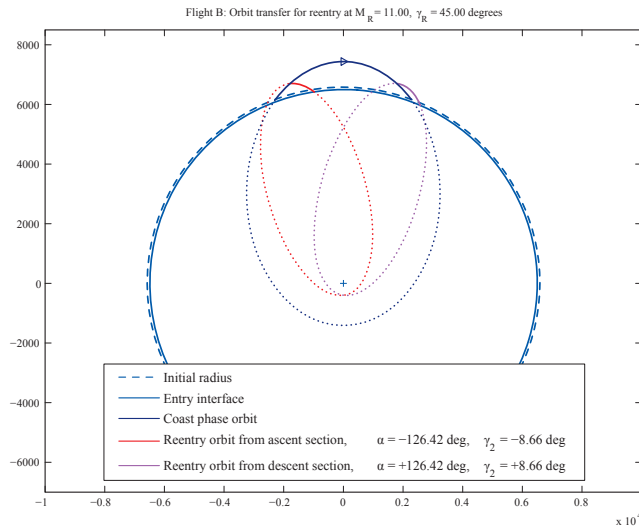


Figure 5. Orbit transfer for  $M_R = 11$  and  $\gamma_R = 45^\circ$ .

**REFERENCES**

Bate, R.R. *et al.*, 1971, “Fundamentals of Astrodynamics”, Dover Publications, Inc., New York, 450p.

Birkhoff, G. and Mac-Lane, S., 1998, “A Survey of Modern Algebra”, AKP Classics, 5th edition, 626p.

Chobotov, V.A., 2002, “Orbital Mechanics”, AIAA Inc., 3rd edition, 460p.

Cornelisse, J.W. *et al.*, 1979, “Rocket Propulsion and Space-flight Dynamics”, Pitman, Belfast, 505p.

Jones, H.L. and Crawford, B. S., 1974, “Space Shuttle Entry and Landing Navigation Analysis”, NASA Tech. Rep. TR-302-2, Houston, Texas, 242p.

Leite Filho, W.C., 1994, “Pointing Algorithm, A Strategy for Orbit Injection with Uncontrolled Last Stage”, In ESA, Proceedings of the 2nd ESA International Conference on GNC, Noordwijk, pp. 339-342.

Nepomuceno, A.L. and Leite Filho, W.C., 2011, “Satellite Launcher Pointing for Orbit Injection with Uncontrolled Solid-Propellant Last Stage”, In: 4<sup>th</sup> European Conference for Aerospace Sciences (EUCASS), July 4-8, Saint Petersburg, Russia.

Pietrobon, H.C. and Leite Filho, W.C., 2011, “Algoritmo de Apontamento para Injeção de Satélite em Órbita”, In: X DINCON Conferência Brasileira de Dinâmica, Controle e Aplicações, 29 de Agosto a 02 de Setembro, Águas de Lindóia.

Robbins, H. M., 1966, “An analytical study of the impulsive approximation”, AIAA Journal, Vol. 4, No. 8, pp. 1417-1423.

Theil, S. *et al.*, 2008, “Hybrid Navigation System for the SHEFEX-2 Mission”, In: AIAA Guidance, Navigation and Control Conference and Exhibit, Honolulu, Hawaii, pp. 1-13.

Thompson, A., 2009, “Edge of Space Found”, Retrieved in April 09, 2009, <http://www.space.com/6564-edge-space.html>.

Weisstein, E.W., 2011, “Cubic Formula.”, From MathWorld – A Wolfram Web Resource, Retrieved in October 15, 2011, <http://mathworld.wolfram.com/CubicFormula.html>.